

# CHIMAERA - The Poly-Magneto-Phonic Theremin - An Expressive Touch-Less Hall-Effect Sensor Array

Hanspeter Portner  
 Open Music Kontrollers  
 Altachenring 5, 4805 Brittnau, Switzerland  
 dev@open-music-kontrollers.ch

## ABSTRACT

The *Chimaera* is a touch-less, expressive, polyphonic and electronic music controller based on magnetic field sensing. An array of linear hall-effect sensors and their vicinity make up a continuous 2D interaction space. The sensors are excited with Neodymium magnets worn on fingers. The device continuously tracks position and vicinity of multiple present magnets along the sensor array to produce event signals accordingly. Apart from the two positional signals, an event also carries the magnetic field polarization, a unique identifier and group association. We like to think of it as a mixed analog/digital offspring of theremin and trautionium. These general-purpose event signals are transmitted and eventually translated to musical events according to custom mappings on a host system.

With its touch-less control (no friction), high update rates (2-4kHz), its quasi-continuous spatial resolution and its low-latency (<1 ms), the *Chimaera* can react to most subtle motions instantaneously and allows for a highly dynamic and expressive play. Its open source design additionally gives the user all possibilities to further tune hardware and firmware to his or her needs. The *Chimaera* is network-oriented and configured with and communicated by Open Sound Control, which makes it straight-forward to integrate into any setup.

## Keywords

Chimaera, touch-less, polyphonic, hall-effect, theremin.

## 1. INTRODUCTION

The main design goals of the *Chimaera* were to have a versatile, easy tunable and modifiable electronic music controller that would give the player optimal control on musical expression. As a prerequisite for an expressive play there is the need to have low-latency access to highly resolved modulation of pitch and timbre of generated sounds and their temporal progression. Pitch and timbre thus would be controllable over continuous ranges with high temporal resolution. Pitch needing a finer control would require a higher resolution and entail a linear controller design.

In its design phase, we required the music controller to be fully hackable, designed for DIY production, entirely based on and released as open source hardware. Setup and com-

munication would be driver-less and based on present networking infrastructure. A combination of distance-sensing (theremin-like [10]) and position-sensing (trautionium-like [8] and ribbon-like [6]) mechanisms served as archetypes for a new digital offspring.

For its musicality, it would be highly sensitive and responsive, accomplished with fast responding sensors running at high update rates (2-4kHz) and low latency (<1ms). We required it to be as expressive as the violin, the theremin and the trautionium while seamlessly being integrable into today's schemes of digital audio synthesis. It would be playable with fingers, as those are among the body parts that we have a very fine grained control on and it would be touch-less and thus circumvent complicating hardware manufacturing.

The design we have come up with that fulfilled all our prerequisites is the *Chimaera* - the poly-magneto-phonic theremin - an expressive touch-less hall-effect sensor array. It is as sensor array that is excitable by an arbitrary number of manually actuated magnetic fields. Depending on where the magnetic fields are located along the array and how near they are to the latter, the device outputs continuous positional event signals which can flexibly be mapped to expressive musical events on a host to drive sound synthesis.

## 2. DESIGN CONSIDERATIONS

### 2.1 Interaction

Up to 160 linear hall-effect sensors aligned on a straight line form the sensory part of the device. Each sensor senses its surrounding magnetic field and outputs a linearly corresponding analog signal [7]. Manually actuated permanent magnets (Neodymium) act as constant mobile magnetic field sources. In our design, each hall-effect sensor thus acts as a miniature theremin and is used for distance-sensing (Fig. 1). Alternative multi sensor theremin-like instruments have previously been built, e.g. with infrared sensors [2]. However, magnetic field sensing has advantages over light and capacitive sensing as it is less susceptible to the surrounding electromagnetic spectrum due to the short-ranged action radius and relative strength of permanent magnets. Linear hall-effect sensors have previously been shown to be practical in building music controllers [3]. Contrasting to other touch-less motion-sensing controllers [11] which are based on moving sensors in a stationary medium (e.g. gravity), the *Chimaera* uses stationary sensors with mobile actuators. As the sensors are narrowly spaced apart, a single magnetic field source is sensed by several adjacent sensors. With continuous tracking and inter-sensor interpolation, vicinity of the magnet to sensors and its exact location along the array can be estimated to a high accuracy (< $\frac{1}{100}$  of inter-sensor distance). The device thus outputs two positional signals for each magnetic field source: position  $x$  and vicinity  $y$ . As sensors are sampled individually, multiple magnets can be tracked concurrently. With

Permission to make digital or hard copies of all or part of this work for personal or classroom use is granted without fee provided that copies are not made or distributed for profit or commercial advantage and that copies bear this notice and the full citation on the first page. To copy otherwise, to republish, to post on servers or to redistribute to lists, requires prior specific permission and/or a fee.

NIME'14, June 30 – July 03, 2014, Goldsmiths, University of London, UK. Copyright remains with the author(s).

magnets worn on fingers (magnetic plectrum) as sources of magnetic fields and varied in their position along and vicinity to the sensor array, the player has touch-less control over a continuous 2D space eventually mapped to a musical expression scheme.

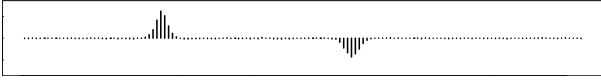


Figure 1: Raw hall-effect sensor dump: Response of two differently polarized Neodymium magnets (144 sensors).

## 2.2 Hardware

The hardware of the *Chimaera* consists of two types of printed circuit boards and an enclosure. Multiple sensor units are daisy-chained to form the sensor array and connected to a single digital signal processing (DSP) unit.

### 2.2.1 Sensor unit

A single sensor unit consists of 16 linear hall-effect sensors spaced 5mm apart and routed to a single output through a 16:1 multiplexer which is switched by the DSP unit. Downstream the multiplexer, the analog signal runs through an amplification circuitry (Fig. 2). To create an equally responding continuous sensor array, all units need equal tuning at their trim potentiometers  $RV_1$ - $RV_3$ .

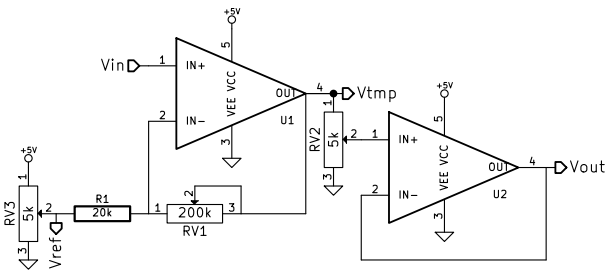


Figure 2: Sensor unit amplification circuitry.

$RV_3$  is a voltage divider to set reference voltage  $V_{ref}$  from  $V_{cc}$  to  $V_{cc}$ . Sensors respond to both north and south polarized magnetic fields and output  $\sim \frac{1}{2}$  of their input voltage (quiescent output) in a zero magnetic field. In a south polarized magnetic field, voltage linearly approaches  $V_{cc}$  and  $V_{cc}$  in a north polarized one. Reference voltage  $V_{ref}$  is set to the mean quiescent voltage of all 16 sensors.

$RV_1$  is a varistor and sets the amplification factor in conjunction with resistor  $R_1$ . The changeable amplification factor  $A = 1 + \frac{RV_1}{R_1}$  accommodates usage of different magnetic field strengths.

$RV_2$  attenuates the signal before handing it over to the DSP unit, a necessity to talk to circuitry running at lower voltages than the sensor unit.

### 2.2.2 Digital signal processing (DSP) unit

The DSP unit is a mixed-signal board and handles sensor read out, event detection and host communication. It is based on an ARM Cortex M4 microcontroller in combination with a hardwired 100Mbit IPv4/PHY chip taking care of all low-level networking protocols via UDP/TCP.

The boards analog part features 10 analog inputs providing connection points for the sensor units, leading to a maximally possible array of 160 sensors. Those analog inputs connect directly to three in parallel running 12bit analog-to-digital converters.

### 2.2.3 Enclosure

The enclosure (Fig. 3) was designed with different playing styles in mind: it can be put flat on a table like a keyboard, strapped around like a guitar or used standing upright like a cello. For its fingered playing style we chose wood for an agreeable touch. The circuitry is embedded in a base rib construction wrapped with a kerf-bent plywood sheet giving a robust, ultra-light construction with rounded edges. The underlying sensors are marked with engravings to ease visual orientation.



Figure 3: Beech enclosure with guitar strap (128 sensors).

## 2.3 Firmware

### 2.3.1 Distance - magnetic field relationship

The strength of magnetic field  $B$  of a permanent magnet along its magnetization axis decreases with increasing distance  $d$  and follows an inverse-cube relationship based on an ideal dipole [7]. The decrease is non-linear dependent on material and physical form.

As we are interested in how near the magnet is to a sensor, we prefer the concept of vicinity ( $y_n = 1 - d$ ). Eqn. 1 adds room for deviations from an ideal dipole and defines normalized vicinity  $y_n$  based on normalized magnetic field  $B_n$ . Vicinity is mapped continuously from  $[0 - 1]$ .  $y = 0$  corresponds to threshold magnetic field  $B_{min}$ ,  $y = 1$  in turn to the maximal to expect magnetic field  $B_{max}$ .  $B_n$  is the measured absolute magnetic field  $B$  normalized in respect to the two extremes (Eqn. 2).

The parameters of the relationship can vary considerably for different types of permanent magnets. The *Chimaera* therefore needs a first calibration step done with a five point least squares fit (Fig. 4a) with points  $(0, 0)$ ,  $(b_1, y_1)$ ,  $(b_2, y_2)$ ,  $(b_3, y_3)$  and  $(1, 1)$  leading to an analytical solution for the three function parameters  $c_0, c_1, c_2$  (Eqn. 3,4). The fitted distance-function then is applied to the sampled magnetic field strength to estimate the corresponding distance in real-time.

$$y_n = c_0 \cdot \sqrt[3]{B_n} + c_1 \cdot \sqrt{B_n} + c_2 \cdot B_n \quad (1)$$

$$B_n = \frac{B - B_{min}}{B_{max} - B_{min}} \quad (2)$$

$$\mathbf{B}_n = \begin{pmatrix} 0 & 0 & 0 \\ \sqrt[3]{b_1} & \sqrt{b_1} & b_1 \\ \sqrt[3]{b_2} & \sqrt{b_2} & b_2 \\ \sqrt[3]{b_3} & \sqrt{b_3} & b_3 \\ 1 & 1 & 1 \end{pmatrix}, \mathbf{Y}_n = \begin{pmatrix} 0 \\ y_1 \\ y_2 \\ y_3 \\ 1 \end{pmatrix} \quad (3)$$

$$\mathbf{C} = \begin{pmatrix} c_0 \\ c_1 \\ c_2 \end{pmatrix} = (\mathbf{B}_n^T \cdot \mathbf{B}_n)^{-1} \cdot \mathbf{B}_n^T \cdot \mathbf{Y}_n \quad (4)$$

### 2.3.2 Sensor comparability

An ideal linear hall-effect sensor outputs a voltage  $V_s$  linearly dependent on its sensitivity  $S$  and magnetic field  $B$  offset by quiescent voltage output  $V_q$  (Eqn. 5). However, both  $V_q$  and  $S$  can vary considerably between sensors due to manufacturing processes [7]. For a successful position and distance interpolation along the sensor array, sensor values must be comparable. We thus need another calibration across sensors to be applied in a normalization step after

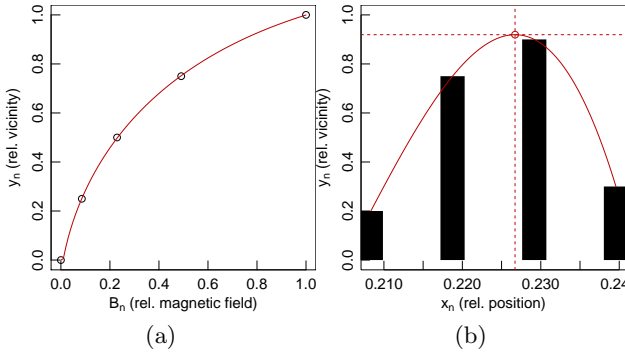


Figure 4: (a) Example distance magnetic field relationship (points) and its least-squares fit (line). (b) Cubic interpolation of position  $x_n$  and vicinity  $y_n$  over four normalized adjacent sensor values with Catmull-Rom splines [1].

sensor read out - a very important concept of *Chimera* inner workings. Amplification of the voltage signal also needs consideration as it varies across individual sensor units.

Amplified voltage output  $V_o$  depends on raw sensor voltage  $V_s$ , reference voltage  $V_r$  and amplification factor  $A$  (Eqn. 6, Fig. 2).  $V_o$  and magnet vicinity are the only variables we can measure directly, all others have to be deduced in the sensor comparability calibration routine. In the case of no magnetic field ( $B = 0$ ), we can measure amplified quiescent voltage  $V_{oq}$  (Eqn. 7) of each sensor from which we can solve for  $V_q$  and rewrite  $V_o$  (Eqn. 8).

$$V_s = V_q + S \cdot B \quad (5)$$

$$V_o = V_r + (V_s - V_r) \cdot A \quad (6)$$

$$V_{oq} = V_r + (V_q - V_r) \cdot A \quad (7)$$

$$V_o = V_{oq} + A \cdot S \cdot B \quad (8)$$

We define a new single parameter  $AS = A \cdot S$  which we calculate over both field polarizations for a higher robustness. Output voltages  $V_{o1}, V_{o2}$  (Eqns. 9-10) are measured for an arbitrary absolute magnetic field strength ( $|B| = |B1| = |B2|$ ), once south polarized and once north polarized ( $B_2 = -B_1$ ). With measured  $V_{oq}$  at  $B = 0$  and  $V_{o1}, V_{o2}$  at the arbitrary  $|B|$ , we can estimate  $AS$  for each individual sensor (Eqn. 11).

$$V_{o1} = V_{oq} + AS \cdot B_1 \quad (9)$$

$$V_{o2} = V_{oq} + AS \cdot B_2 \quad (10)$$

$$AS = \frac{V_{oq} \cdot (V_{o1} - V_{o2})}{|B| \cdot (V_{o1} + V_{o2})} \quad (11)$$

$|B|$  cannot be measured directly, instead we approximate it numerically with the inverse of the previously calibrated distance - magnetic field relationship (Eqn. 1, Fig. 4a).  $|B|$  ultimately depends on three constants  $V_{oq}, U$  (Eqn. 12) and  $W$  (Eqn. 13).  $V_{oq}$  and  $U$  are specific to each sensor,  $W$  is constant for the whole sensor array. Thus we directly get from raw sensor voltage output  $V_o$  over normalized magnetic field strength  $B_n$  (Eqn. 14) to normalized vicinity  $y_n$  (Eqn. 1). With vicinities being comparable over the whole sensor array, only now we are able to interpolate position  $x_n$  of the magnets along the array.

$$U = (AS \cdot (B_{max} - B_{min}))^{-1} \quad (12)$$

$$W = B_{min} \cdot (B_{max} - B_{min})^{-1} \quad (13)$$

$$B_n = (V_o - V_{oq}) \cdot U - W \quad (14)$$

### 2.3.3 Blob event handling

A blob represents a recognized magnetic permanent magnet that is to be tracked over space and time. Blob event handling is divided into the following stages:

**Magnetic flux polarity** Firstly, we discriminate between the polarities of the potentially present magnetic field sources. For each raw sensor read out  $V_o$  we subtract its previously calibrated quiescent value  $V_{oq}$ . The sign of the difference corresponds to the polarity, the absolute value  $|V_o - V_{oq}|$  in turn to the strength of the magnetic field.

**Area of interest** After each scan of the whole sensor array, areas of interest are marked on the array where sensor values exceed their threshold  $B_{min}$ . The rest of the sensor values are not of interest for further steps.

**Blob detection** A peak in the sensor read out marks an individual magnetic field source and is located around a sensor with an absolute value greater than the values of a given number of adjacent sensors in the same area of interest (Fig. 4b).

**Blob interpolation** As always more than one sensor is excited by an individual magnetic field source, its real position can be deciphered by interpolation around the peak sensor. We fit linear, quadratic, cubic or spline curves (Eqn. 15, Fig. 4b) through adjacent sensor values and find the current position  $X_n$  along the sensor array and vicinity  $Y_n$  by finding the cross point of the curve's derivative (Eqn. 16).

$$y_n(x_n) = \sum_{j=0}^{1,2,3} x_n^j \cdot m_j \quad (15)$$

$$y_n(X_n) = Y_n \quad , \quad \frac{\partial y_n(X_n)}{\partial x_n} = 0 \quad (16)$$

**Group association** Each blob additionally gets affiliated to a group defined by a range  $[x_{min} - x_{max}]$  on the sensor array and magnetic field polarity south, north or both. Only blobs with a position in the range of - and a polarity corresponding to - a given group will be associated with the latter. Groups may overlap but a given blob can only be part of one group at a time.

**Blob tracking** To track blobs over time, we need to associate identified blobs in the current iteration step to blobs found in previous iteration steps to decipher whether blobs have newly appeared, need updating or have disappeared. To link current blobs to previous blobs they are matched by position on the sensor array across iteration steps. Each new blob gets a unique ID, which persists over time as long as the blobs position and field polarity can be linked to itself in a previous iteration step.

Out of the blob tracking we get a stream of event signals: When a new blob has appeared, an *ON* event is triggered. When a blob was present in a previous iteration step, a *SET* event is triggered to update the blobs position and vicinity. When a blob has disappeared, an *OFF* event is triggered. All event signals will be triggered with a complete set of current blob parameters including polarity (south or north) and group association.

## 2.4 Communication

Networking technology in a zero configuration setup [9] has advantages in respect to long-distance transmission, operating system independence and inherent ability for network

performances. We thus use the Open Sound Control (OSC) specification [12] via UDP/TCP as low-level communication layer. UDP is preferable in simple setups due to its better real-time performance, whereas we prefer TCP in more complex and/or lossy (e.g. wireless) setups.

Depending on the robustness of the network connection we provide different higher-level protocols built on top of OSC. Those are implemented as output engines of the blob-tracking procedure. An arbitrary amount of engines can be active concurrently as they are aggregated into one single timestamped OSC bundle after each iteration step. Time synchronization to the host is based on the precision time protocol [4]. The user can implement custom protocols if the existing ones should not fit his or her needs. As main protocol for lossy connections, we use the *TUIO* specification [5] because it is widely used and unsusceptible to lost network packets. Apart from a direct serialization of the event stream and standard MIDI via OSC on lossless communication channels, the device also supports a raw sensor dump for further manual processing.

## 2.5 Musicality

The receiving host can reconstruct which blobs have appeared, disappeared or need updating. These polyphonic event signals can be combined in any way possible, it is up to the host to map them to musical events.

A trivial mapping approach e.g. is to steer one sound unit per blob and initiate it at an *ON* event, update its properties at each *SET* event and stop the unit at an *OFF* event. Position having a higher resolution than vicinity is predestined to map to pitch. The event stream thus can directly be translated to MIDI using position mapped to note and pitch bend and vicinity mapped to MIDI controller events (volume, modulation, polyphonic after touch, ...).

The two continuous signals need not be mapped directly to a control parameter though, we can additionally derive velocity and acceleration signals to derive augmented mappings or feed gestural responders. By aggregating multiple blobs into compounds, a single sound unit can be controlled with multiple degrees of freedom, giving the player an even more fine grained control on musical expression.

The high spatial and temporal resolution make it possible to play a subtle vibrato and tremolo and intermix a percussive play with continuous (pitch) slides.

## 2.6 Ergonomy

For an expressive and melodic play, we prefer to play touchless by hovering along and perpendicular to the sensor array similar to the theremin play, just with an additional dimension and polyphony. When playing percussive, it helps to have a haptic feedback. To better coordinate rhythmic play, we thus tap on the surface and adjust magnet vicinity by finger curvature. While tapping, due to the touch-less design, events and thus sound synthesis are triggered before reaching the surface, but we did not find this to be distracting and barely noticeable as the effect is eventually offset by network and audio delays.

The device needs some practice to master. The continuous scale demands a constant feedback between hearing and positional micro adjustments. Muscle memory needs to be trained like with fretless string instruments and coordination of multiple magnets even more so.

We consider two plectra as the maximum for one hand and best to be worn on fingers not adjacent to each other as magnets tend to stick together. Although both magnets have two degrees of freedom, the second one will be reduced in its freedom to move along the sensor array as fingers can only be stretched apart for a fixed distance and the

muscles involved usually are not well trained. The absolute positional signal of the second magnet thus is of minor use, it makes more sense to use its position relative to the first magnet instead. Two magnets on one hand can also be combined to form a unit to decipher position, vicinity and angle of the whole hand. Four concurrent plectra for a single player with eight degrees of freedom are thus feasible with the current design.

## 3. CONCLUSIONS

The *Chimaera* is an open, expressive, electronic music controller combining both distance-sensing (theremin-like) and touch-less position-sensing (trautonium-like) with a fully digitized, portable, network-ready event output stream suitable for a dynamic and expressive play. By freely combining the polyphonic event signals, the player can create augmented, multi dimensional musical mappings.

Our design could be extended to a third dimension by interpolating across at least three parallel sensor arrays to gain an additional degree of freedom per plectrum.

## 4. ACKNOWLEDGMENTS

We thank LeafLabs for their open hardware and software designs this project is based on and our beloved ones for their endless patience.

## 5. REFERENCES

- [1] E. Catmull and R. Rom. A class of local interpolating splines. *Computer aided geometric design*, 74:317–326, 1974.
- [2] I. Franco. The AirStick: a free-gesture controller using infrared sensing. In *Proceedings of NIME'05*, pages 248–249, Singapore, 2005.
- [3] L. Haken, E. Tellman, and P. Wolfe. An indiscrete music keyboard. *Computer Music Journal*, 22(1):30–48, 1998.
- [4] IEEE Std 1588-2008. IEEE standard for a precision clock synchronization protocol for networked measurement and control systems, 2008.
- [5] M. Kaltenbrunner, T. Bovermann, R. Bencina, and E. Costanza. TUIO - a protocol for table based tangible user interfaces. In *Proceedings of the Workshop on Gesture in Human-Computer Interaction and Simulation*, Vannes, 2005.
- [6] J. Paradiso. Electronic music: new ways to play. *IEEE Spectrum*, 34(12):18–30, 1997.
- [7] E. Ramsden. *Hall-Effect Sensors: Theory and Application*. Newnes, 2011.
- [8] O. Sala. Experimentelle und theoretische grundlagen des trautoniums. *Frequenz*, 3(1):13–19, 1949.
- [9] D. H. Steinberg and S. Cheshire. *Zero configuration networking: The definitive guide*. O'reilly, 2010.
- [10] L. Theremin. Method of and apparatus for the generation of sounds, 1928. Patent. US1661058 A.
- [11] G. Vigiensoni and M. M. Wanderley. A quantitative comparison of position trackers for the development of a touch-less musical interface. In *Proceedings of NIME'12*, Vancouver, 2012.
- [12] M. Wright. Open sound control: an enabling technology for musical networking. *Organised Sound*, 10(03):193–200, 2005.

## APPENDIX

The *Chimaera* is open source hardware released under CERN OHL v.1.2. <http://open-music-kontrollers.ch/chimaera/>